ENHANCING LAND COVER MAPPING: A NOVEL AUTOMATIC APPROACH TO IMPROVE MIXED SPECTRAL PIXEL CLASSIFICATION

Surbhi Sharma[1,2], *Rocco Sedona*[2], *Morris Riedel*[1,2], *Gabriele Cavallaro*[1,2], *Claudia Paris*[3]

[1]School of Engineering and Natural Sciences, University of Iceland, 107 Reykjavik, Iceland
[2]Jülich Supercomputing Centre, Forschungszentrum Jülich, 52428 Jülich, Germany
[3]University of Twente, 7514 AE Enschede, The Netherlands

ABSTRACT

The increasing availability of high-resolution, open-access satellite data facilitates the production of global Land Cover (LC) maps, an essential source of information for managing and monitoring natural and human-induced processes. However, the accuracy of the obtained LC maps can be affected by the discrepancy between the spatial resolution of the satellite images and the extent of the LC present in the scene. Indeed, several pixels may be misclassified because of their mixed spectral signatures, i.e., more than two LC classes are present in the pixel. To solve this problem, this paper proposes an approach that explores the possibility of using simple but effective unmixing approaches to enhance the classification accuracy of the mixed spectral pixels. The results showed that several pixels, including buildings and grassland LC, are typically classified as cropland. By unmixing their spectral content, it is possible to extract the most prevalent class within the area of each pixel to update the classification map, thus sharply increasing the map accuracy. These promising preliminary results indicate the potential for broader applicability and efficiency in global LC mapping.

Index Terms— Land Cover (LC) mapping, spectral unmixing, Sentinel-2, Land use/cover area frame survey (LUCAS).

1. INTRODUCTION

With the Copernicus Programme, the availability of free and open high-resolution satellite data has completely transformed the methods used to monitor the Earth's surface. The spatial, temporal, and unique spectral properties of the Copernicus Sentinel-2 satellite data have enabled the Earth observation (EO) community to produce global thematic products at a 10m spatial resolution [1]. The production of accurate LC maps enables continuous monitoring of the Earth's surface, which is crucial for managing the planet's resources and observing environmental processes such as desertification, urbanization, and deforestation [2].

Multiple satellite pixels can be associated with mixed spectral signatures due to the differing spatial resolutions of satellite images compared to the extent of the LC classes present in the scene. This can lead to inaccurate classification results, thus affecting the reliability of the final thematic product [3]. In [4], the authors demonstrated that when evaluating the accuracy of existing thematic products using validation databases derived by visually interpreting satellite data, they achieved higher accuracy than when using *in-situ* data. This discrepancy typically occurs when the size of the LC class present in the scene is much smaller than the geometrical resolution of the satellite data, e.g., small rivers or tiny roads [3]. While much effort has been devoted to generating LC products at the global level [4], little has been done to mitigate the influence of mixed pixels on the LC classification result [5].

To solve this problem, the main objective of this paper is to understand and deal with the complexities of specific LC classes at a pixel level to increase the accuracy of obtained LC maps, using spectral unmixing with underlying semantic differences. First, a pre-processing step performs data harmonization of the considered time series of optical satellite data. Then, an ensemble of Random Forest (RF) classifiers is trained to produce a set of LC maps that are compared to detect discrepancies among them. This condition allows to automatically detect the samples with the highest probability of belonging to mixed spectral pixels, i.e., those with inconsistent classification results. Finally, for the inconsistent pixels, a state-of-the-art unmixing approach is applied to disentangle the different spectral components and determine the best LC label to be assigned to those pixels.

2. PROPOSED METHOD

Fig. 1 shows the block diagram of the proposed method, which is based on three main steps: (i) satellite data pre-

The research leading to these results was conducted within the ADMIRE project, which received funding from the European Union's Horizon 2020 JTI-EuroHPC research and innovation programme under grant agreement No. 956748. This work also received complementary funding from the German Federal Ministry of Education and Research under grant No. 16HPC008. This work is co-financed by the EUROCC2 project funded by the European High-Performance Computing Joint Undertaking (JU) and EU/EEA states under grant agreement No. 101101903.

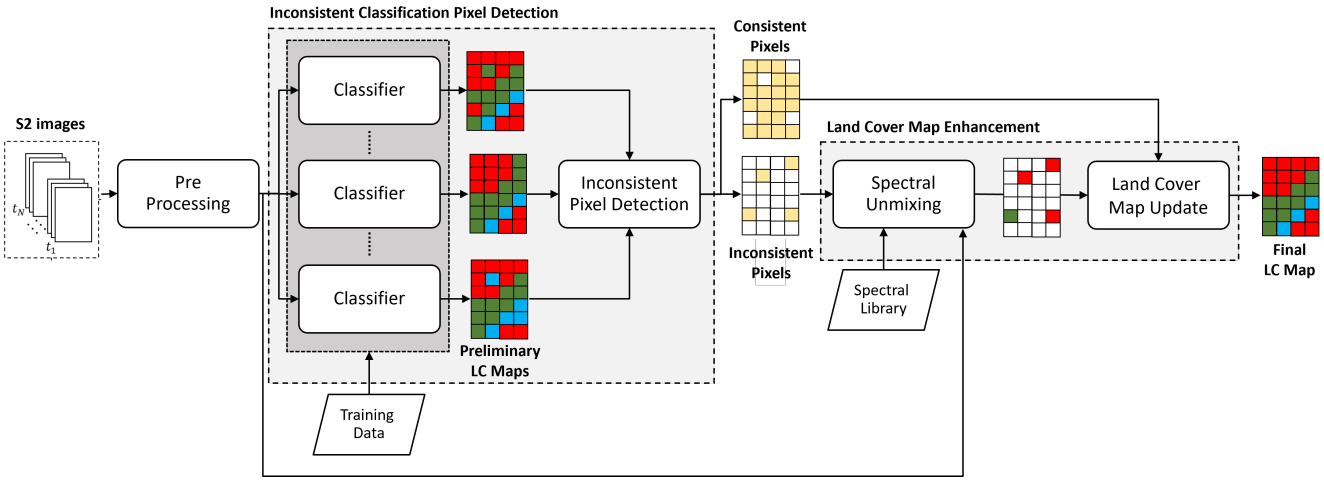

Fig. 1. Workflow of the proposed data-driven approach to improve LC mapping of the mixed spectral pixels.

processing, (ii) identification of inconsistent LC classification results, and (iii) LC map enhancement for mixed spectral pixels.

2.1. Pre-processing

In the first step of the proposed method, the time series of optical satellite images used to generate the LC map are harmonized. In the considered experiments, the Sentinel-2 satellite data, widely used for LC mapping due to their high spatial resolution (10m), high revisit time (up to 5 days), and spectral properties, are utilized [4, 6]. In particular, a time series of Sentinel-2 images acquired throughout the year is considered to generate an annual LC map. To remove cloud coverage and harmonize the data from the spatial and temporal viewpoint, the time series of images are converted into a time series of 12 monthly composites. The median approximation of the reflectance values collected over each month is computed for each pixel. Let $\mathbf{TS} = (\mathbf{X}_1, \mathbf{X}_2, \cdots, \mathbf{X}_{12})$ be the time series of 12 monthly composites, with $\mathbf{x}_k \in \mathbb{R}^{1\times 120}$ representing the kth pixel's temporal spectral vectors associated with the 120 features, i.e., 10 reflectance values $\times$ 12 months. These monthly composites are then used to generate LC maps.

2.2. Inconsistent Classification Pixel Detection

The second step of the proposed method aims to automatically identify the mixed spectral pixels with the highest probability of being misclassified. To this end, an ensemble of statistically independent Random Forest classifiers is trained using randomly chosen training samples via a bootstrap technique [7, 8]. Let Ω_c be the set of LC classes present in the scene. The initial pool of labeled data is sampled without replacement to generate of N training set, i.e., $\{T_1, T_2, \cdots, T_N\}$ used to train N independent classifiers $\{C_1, C_2, \cdots, C_N\}$, where $T_n = \{(\mathbf{x}_b, y_b)\}_b$ is the nth training set having $\mathbf{x}_b \in \mathbb{R}^{1\times 120}$ and $y_b \in \Omega_c$. In this setup, it is reasonable to assume that the obtained classification errors are uncorrelated and associated with the mixed spectral pixels, which typically lead to uncertain classification results. By comparing the ensemble of obtained LC maps, the pool of inconsistent pixels having the highest probability of being mixed from the spectral viewpoint is identified.

2.3. Land Cover Map Enhancement

Finally, the method aims to identify inconsistencies and misclassifications that provide patterns and information about mixed pixels. Here, for simplicity, we used Linear Spectral Unmixing to analyze the contribution of different endmembers, or materials within a mixed pixel [9]. However, any other unmixing techniques can be considered. The linear mixing model is often represented as follows:

$$R = S \cdot A + E, \tag{1}$$

where: R represents the observed spectrum of a mixed pixel, S is a matrix containing the spectra of the endmembers, A is a vector containing the abundance fractions of each endmember in the pixel, and E is an error term accounting for factors such as noise or atmospheric effects. The objective of spectral unmixing is to determine the abundance fractions (A) of each endmember within a mixed pixel. An abundance map illustrates the spatial distribution of these fractions throughout an image. These abundance maps are generated on the yearly composite of Sentinel-2 time-series images obtained by using the median approximation of the reflectance values collected over the whole year for each pixel. These maps are further used to improve classification accuracy by updating LC maps with the most prevalent class.

3. DATASET DESCRIPTION

To train and validate the obtained LC map, we used *in-situ* data from the Land Use and Coverage Area frame Sur-

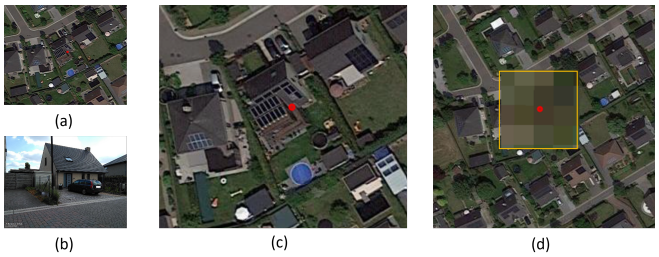

Fig. 2. Example of LUCAS point labeled as 'Artificial Land' (a) High-resolution Google Earth Satellite View, (b) LUCAS street-level image, (c) zoomed-in view of the residential area containing LUCAS point, (d) Sentinel-2 image located in the LUCAS point.

vey (LUCAS) database [10], a survey coordinated by the Statistical Office of the European Commission (Eurostat), which collects harmonized data on land cover/land use, agro-environmental variables, and soil through field observation of geographically referenced points. The LC labels in the LUCAS database are defined according to the Land Cover Classification System (LCCS) [11].

The experimental setup preprocesses and downloads time series of Sentinel-2 Level-2A data for 2018. Each series consists of a 3×3 pixel patch with a $20\,\mathrm{m}$ spatial resolution (discarding bands with a $60\,\mathrm{m}$ spatial resolution) and is associated with the LC label available in LUCAS. To capture a detailed and accurate representation of ground reference data, a 3×3 patch of Sentinel-2 is used. As an example in Fig. 2, it can be seen that even though the LUCAS point clearly describes a residential area to be classified as artificial land (see Fig. 2(a), Fig. 2(b), and Fig. 2(c)), the Sentinel-2 pixel associated with the point location is mixed (see Fig. 2(d)), covering a grassland as well, potentially leading to a mixed spectral signature and misclassification.

4. EXPERIMENTS AND RESULTS

To assess the effectiveness of the proposed approach, results have been carried out at the country and continental level. In particular, we considered 3659 LUCAS points from Belgium and 337854 LUCAS points covering the European Union (EU). A pool of inconsistent pixels was identified by comparing the ensemble of LC maps obtained using the RF classifier, having the highest probability of being mixed as described in Section 2.2. The class probabilities per pixel were also calculated for 9 LC classes, namely 'Artificial land', 'Bareland', 'Broadleaves', 'Conifers', 'Cropland', 'Grassland', 'Shrubland', 'Water', and 'Wetland'. A total of 478 pixels from Belgium and 51,806 pixels from EU with a higher class probability of being in more than one class were identified as mixed and chosen for further spectral analysis. From the obtained inconsistent samples, 220 samples from Belgium and 26,316 samples from EU are found to be misclassified.

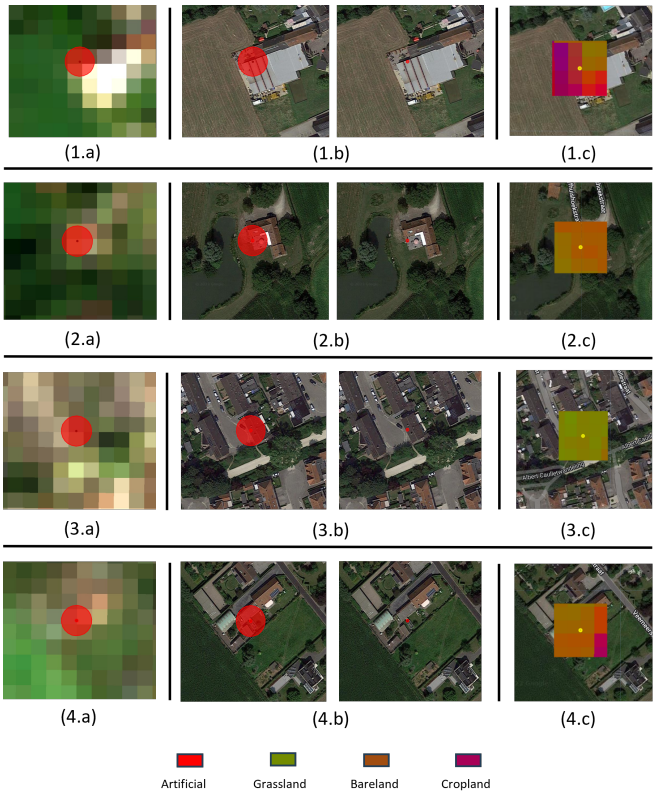

Fig. 3. Abundance Map obtained after Spectral Unmixing for four different LUCAS points, marked as red and yellow, labeled as 'Artificial Land'. Figures (1.a)-(4.a) and (1.b)-(4.b) show the LUCAS points in Sentinel-2 and High-resolution Google Earth Satellite View. Figures (1.c) - (4.c) represent the Abundance Map obtained from the Sentinel-2 yearly composite of respective LUCAS points.

For experimentation, our study is limited to 478 pixels from Belgium and a randomly selected subset of 1000 pixels out of 51,806 inconsistent pixels from the EU to reduce the overall computational time.

Fig. 3 shows example cases corresponding to four different LUCAS points labeled as 'Artificial land'. Since the obtained inconsistent pixels belong to some of the major LC classes, the abundance maps were created by performing spectral unmixing, focusing on finding 9 major classes, namely 'Artificial land', 'Bareland', 'Broadleaves', 'Conifers', 'Cropland', 'Grassland', 'Shrubland', 'Water', and 'Wetland' as shown in Fig. 3. These maps are created on a 3×3 patch for a more detailed and optimal view of what is on the ground using the annual composite, as shown in Fig. 3(1.c) - (4.c), respectively. The endmembers, or the 'pure spectra', were determined in a supervised way for the purpose of cross-referencing. Finally, the labels were updated based on the highest abundance fraction of the class obtained.

The overall classification accuracy and weighted average

Table 1. The weighted average F-score and Overall accuracy using the baseline and proposed method.

Classes	Belgium		Samples from EU	
	Baseline	**Proposed Method**	**Baseline**	**Proposed Method**
Weighted Average F1-score	0.51	0.63	0.43	0.54
Overall Accuracy	0.54	0.62	0.45	0.54

F1-score for the baseline method and our proposed method, are reported in Tab. 1. It can be seen that our proposed methodology performs well overall. The results obtained on a single country, Belgium, and at the European level suggest that assigning the pixels to the class corresponding to the highest abundance fraction can help improve the accuracies of LC classification.

5. CONCLUSION

This paper introduces a data-driven workflow for improving LC maps via spectral unmixing, specifically targeting mixed pixel issues to bolster classification accuracy. This study makes use of an automated workflow and method to generate abundance maps and update LC labels using optimized resources available on High-performance computing (HPC) systems and data parallel processing strategies. The results suggest potential for streamlining both the LC classification and enhancement processes. The study also explores the misclassification arising from semantic differences between satellite and *in-situ* data, which are attributed to their different spatial resolutions and viewpoints. The obtained results provide insights into the mixed spectral classes that are typically present at a scene and are misclassified. With the help of spectral unmixing, the proposed approach successfully updates the classification maps by extracting the most prevalent class within the area of each pixel, increasing the accuracy of the LC map.

6. FUTURE DEVELOPMENTS

The obtained abundance fractions provide valuable insights for the most prevalent class present on the scene. In cases where the highest abundance fractions do not match or justify the *in-situ* data, especially where the second abundance fraction is the actual class label, a detailed analysis of each time series component from patches and rule-based filtering can be opted for updating LC labels. In addition, advanced Deep Learning (DL) models, known for their extensive data requirements, such as Transformers, could significantly enhance the accuracy of baseline methods like RF [12]. Other unsupervised techniques for evaluating endmembers, such as Vertex Component analysis (VCA), also hold the potential for significantly expediting the workflow, which, on the other hand, relies mostly on the spectral disposition of the dataset [13, 14].

7. REFERENCES

[1] R. Van De Kerchove, D. Zanaga, W. Keersmaecker, N. Souverijns, J. Wevers, C. Brockmann, A. Grosu, A. Paccini, O. Cartus, M. Santoro, et al., "Esa worldcover: Global land cover mapping at 10 m resolution for 2020 based on sentinel-1 and 2 data.," in *AGU Fall Meeting Abstracts*, 2021, vol. 2021, pp. GC45I–0915.

[2] A. Stoian, V. Poulain, J. Inglada, V. Poughon, and D. Derksen, "Land cover maps production with high resolution satellite image time series and convolutional neural networks: Adaptations and limits for operational systems," *Remote Sensing*, vol. 11, no. 17, pp. 1986, 2019.

[3] C. Paris, L. Martinez-Sanchez, M. van der Velde, S. Sharma, R. Sedona, and G. Cavallaro, "Accuracy assessment of land-use-land-cover maps: the semantic gap between in situ and satellite data," in *Image and Signal Processing for Remote Sensing XXIX*. 2023, vol. 12733, SPIE.

[4] Zander S Venter, David N Barton, Tirthankar Chakraborty, Trond Simensen, and Geethen Singh, "Global 10 m land use land cover datasets: A comparison of dynamic world, world cover and esri land cover," *Remote Sensing*, vol. 14, no. 16, pp. 4101, 2022.

[5] Chao Yang, Guofeng Wu, Kai Ding, Tiezhu Shi, Qingquan Li, and Jinliang Wang, "Improving land use/land cover classification by integrating pixel unmixing and decision tree methods," *Remote Sensing*, vol. 9, no. 12, pp. 1222, 2017.

[6] European Space Agency (ESA), "Copernicus Sentinel-2 MSI Level-2A BOA Reflectance Product," 2021, Collection 1.

[7] L. Breiman, "Random forests," *Machine Learning*, vol. 45, pp. 5–32, 2001.

[8] Gilles Louppe, "Understanding random forests: From theory to practice," 2015.

[9] Jiaojiao Wei and Xiaofei Wang, "An overview on linear unmixing of hyperspectral data," *Mathematical Problems in Engineering*, vol. 2020, pp. 1–12, 08 2020.

[10] R. d'Andrimont, M. Yordanov, L. Martinez-Sanchez, B. Eiselt, A. Palmieri, P. Dominici, F. J. Gallego Pinilla, H. Reuter, C. Joebges, G. Lemoine, and M. Velde, "Harmonised lucas in-situ land cover and use database for field surveys from 2006 to 2018 in the european union," *Scientific Data*, vol. 7, 10 2020.

[11] M. Herold, R. Hubald, and A. Di Gregorio, "Translating and evaluating land cover legends using the un land cover classification system (lccs)," *GOGC-GOLD Report*, vol. 43, 2009.

[12] Ashish Vaswani, Noam Shazeer, Niki Parmar, Jakob Uszkoreit, Llion Jones, Aidan N. Gomez, Lukasz Kaiser, and Illia Polosukhin, "Attention is all you need," *CoRR*, vol. abs/1706.03762, 2017.

[13] J.M.P. Nascimento and J.M.B. Dias, "Vertex component analysis: a fast algorithm to unmix hyperspectral data," *IEEE Transactions on Geoscience and Remote Sensing*, vol. 43, no. 4, pp. 898–910, 2005.

[14] José M. Rodríguez Alves, José M. P. Nascimento, José M. Bioucas-Dias, Vítor Silva, and Antonio Plaza, "Parallel implementation of vertex component analysis for hyperspectral endmember extraction," in *2012 IEEE International Geoscience and Remote Sensing Symposium*, 2012, pp. 4078–4081.